

Timestamp-independent Haptic-Visual Synchronization

Yiwen Xu
xu_yiwen@fzu.edu.cn
Fuzhou University

Liangtao Huang
211120101@fzu.edu.cn
Fuzhou University

Tiesong Zhao
t.zhao@fzu.edu.cn
Fuzhou University

Liqun Lin
lin_liqun@fzu.edu.cn
Fuzhou University

Ying Fang
fy@fzu.edu.cn
Fuzhou University

ABSTRACT

The booming haptic data significantly improves the users' immersion during multimedia interaction. As a result, the study of Haptic, Audio-Visual Environment (HAVE) has attracted attentions of multimedia community. To realize such a system, a challenging task is the synchronization of multiple sensorial signals that is critical to user experience. Despite of audio-visual synchronization efforts, there is still a lack of haptic-aware multimedia synchronization model. In this work, we propose a timestamp-independent synchronization for haptic-visual signal transmission. First, we exploit the sequential correlations during delivery and playback of a haptic-visual communication system. Second, we develop a key sample extraction of haptic signals based on the force feedback characteristics, and a key frame extraction of visual signals based on deep object detection. Third, we combine the key samples and frames to synchronize the corresponding haptic-visual signals. Without timestamps in signal flow, the proposed method is still effective and more robust to complicated network conditions. Subjective evaluation also shows a significant improvement of user experience with the proposed method.

KEYWORDS

Haptic Audio-Visual Environment (HAVE), multimedia environment, human-centric multimedia, haptics, haptic-visual synchronization

1 INTRODUCTION

The recent developments of multimedia technology also cultivate the user requirements on multimedia contents that a more immersive multimedia system is imperative. As an emerging multimedia signal, the haptics provides newfangled and authentic user perception beyond the reigning audio-visual signals. Thus, the Haptic, Audio-Visual Environment (HAVE) has raised concerns of researchers with widespread applications in remote surgery, remote training/education, etc [1, 2, 16, 21].

Similar to conventional audio-visual signals, the haptic signal can also be affected during network fluctuations or congestions. In multimedia case, the haptic signal may lose synchronization with other signals, e.g. images, videos. As reported, the haptic-visual asynchronization greatly influences the user experience. Qi et al. [28] implemented several experiments to explore the impact of the delay between video and haptic signals on the quality of users' experience. The results showed that all the Mean Opinion Score (MOS) values decreased with the inter-flow synchronization

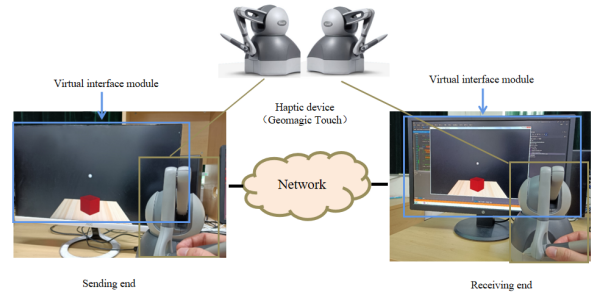


Figure 1: Our simulation platform for haptic-visual signal delivery

error. The works from Aung et al. [3] also confirmed the above conclusion.

To address this issue, the haptic-visual synchronization is desired. The system examines the synchronization status of signals in real time and adjusts the corresponding signals immediately when an asynchronization is found. To our best knowledge, there is still a lack of synchronization method that is designed for haptic-visual signals, although we have seen enormous models for audio-visual asynchronization detection. In the state-of-the-art HAVE systems, the haptic-visual synchronization is achieved by the timestamp method [7, 19] that was designed for generic signals. The timestamp-dependent method embeds the timestamps in signal stream to avoid synchronization drift. The receiving-end detects the signal synchronization status based on the timestamps and the system clock. However, the timestamp-dependent method has its drawbacks. Firstly, in sending end, the timestamps are usually added after frame synchronization, format conversion or pre-processing, where the delay derived from these operations are not compensated [19]. Thus this signal asynchronization in sending end will take to and always exist in the receiving end. Secondly, as the sending and receiving ends have different system clocks (the same frequency), the initial delay and frequency offset caused by dynamic environments also lead to signal asynchronization.

In this paper, we propose a first-of-its-kind timestamp-independent synchronization method for haptic-visual signals. There exists a strong sequential correlation between haptic-visual signals, which can help the judgment of signal synchronization state without crystal oscillators or timestamps. Inspired by this, we propose a timestamp-independent haptic-visual synchronization model that successfully detect and eliminate asynchronization phenomena in

our simulation platform in Fig. 1. Our contributions are summarized as follows.

The sequential correlation between haptic-visual signals. We build a multimedia communication platform with both haptic and visual signals, based on which we observe a strong correlation between the two signals during haptic-aware interaction. This intrinsic correlation is further utilized to design our synchronization model.

The key sample/frame extraction during haptic-visual interaction. We exploit the statistical features of haptic-visual signals and then develop learning-based methods to extract key samples and key frames in haptic and visual signals, respectively.

The asynchronization detection and removal strategy. Combing the correlation and key samples/frames, we are able to detect and eliminate asynchronization when the registration delay is larger than a threshold. Experimental results with subjective evaluations validate the effectiveness of our method.

2 RELATED WORK

Haptic-based interaction. Introducing haptics into the process of human-computer interaction can effectively improve the immersion and realism of the multimedia system, hence, researchers have been conducting research on Haptic-based Interaction System (HIS) since the 1990s [25]. The work in [18] proposed a typical HIS framework, which consists of a master control end, a network, and a controlled end. The master control end usually consists of an haptic operator and a human-computer interaction module, which implements the acquisition and pre-processing of haptic signal and transmits them to the controlled end via the network. In the controlled end, a remotely controlled robot or a controlled operator executes the remote interaction commands from the main control end, and at the same time feeds the scene information to the main control end. Our haptic-based simulation platform presented in Section 3 is also according to the above framework.

HIS has been used in a variety of applications. Ilaria et al. [11] designed an immersive haptic VR system for rehabilitation training of children with motor neurological disorders, which significantly improved the effect of rehabilitation training. Zhou et al. [29] proposed an approach with visual and haptic signals, which help physicians to perform surgeries accurately and effectively and furthermore reduce their physical and cognitive burden during surgery. Chen et al. [5] designed a remote training system with force feedback for power grid operation training. It avoided the collision between the manipulator and steel bars, which helps guide operators to reduce operational errors and complete tasks efficiently. Varun et al. [6] also introduced haptics into a VR-based training system to enhance training immersion, effectiveness and efficiency. The use of HIS for online shopping [9, 10] can improve the realism of the shopping experience and help visually impaired patients enjoy the convenience of online shopping. HIS can also be used in outdoor search and rescue scenarios to avoid collisions by providing tactile guidance [15]. In industry, HIS is usually used to enhance the operation ability of robots. For example, the work in [8] equipped robot with bionic haptic manipulators to help it having more stable grasping ability in teleoperation tasks. In [14], the operator controls the robot to perform teleoperation in real time by means of a pneumatic haptic

feedback glove. Apparently, the HIS is widely used and worthy of further investigation.

Haptic-based transmission and synchronization. Haptic interaction enables real-time perception, manipulation and control of real or virtual objects. Compared to video, audio, or image, the transmission of haptics is more tolerant of data loss and bandwidth but has higher requirements for the latency between signals. To ensure more natural interactive operations, haptic-based multimedia signal transmission requires better inter-signal synchronization. However, to the best of our knowledge, current research on synchronization of visual-haptic signals is mainly focused on studying the impact of visual-haptic asynchronization on user experience, while few research has been conducted on synchronization detection and adjustment of visual-haptic signals, and there is still room for improvement in this area.

The researches on synchronization algorithms for audio-visual signals can be used as good references for the research on visual-haptic signals. Timestamp-dependent synchronization method is the most commonly used audio-visual synchronization method (and the method is currently adopted by the video-haptic system), but the method has some shortcomings (summarized in Section 1). To solve these shortcomings, researchers have proposed some improvement algorithms. For example, the works in [12, 23] utilized the correlation between audio-visual signals for synchronization detection. They extract lip pictures in video frames and then compare them with the features of audio signal through a deep-learning-based model to determine the synchronization status of audio-visual signals. The limitation of this method is that the video frame must contain the lip region. Yang et al. [26] proposed a watermark-based method to keep the synchronization of audio-visual signal. But this method have a disadvantage that the "watermark" is not well adapted to the video or audio signal when applying conversion, aspect ratio conversion or audio downmixing [20]. In the work of [17], the features of the audio and visual signals are converted into robust hash codes. At the receiving end, the received signal is used to generate the "signature" again and compare it with the received "signature" to obtain the inter-stream delay of the audio-visual signal.

The asynchronization may occur during the transmission and decoding recovery of multimedia signals due to various factors such as network environment and clock drift. Obviously, signal asynchronization can greatly affect the quality of user experience, so when it occurs, an removal algorithm should be adopted to remove the asynchronization. In this work, we have addressed both asynchronization detection and removal of haptic-visual signals with deep learning. The detailed motivation and explanation of our method is discussed as follows.

3 HAPTIC-VISUAL CORRELATIONS

To design and test our haptic-visual synchronization method, we build a simulation platform with haptic-visual signal delivery. As shown in Fig. 1, we use the virtual interaction module to design a haptic-visual interaction scenario, where a human user manipulates a virtual ball to push a virtual box. A Geomagic Touch is deployed to connect the real and virtual world: on one hand, it sends the human instructions to the virtual ball; on the other hand, it collects

the force feedback of the virtual ball and sends the corresponding signals back to the human user. This haptic interaction is achieved with the kinesthetic signal, which is a major component of haptic information.

Besides of the haptic signals captured by Geomagic Touch, the sending-end also records the visual contents of virtual space, resulting in a high-definition video at a resolution of 1920×1080 . Then the video is compressed by High Efficiency Video Coding (HEVC) and subsequently delivered with haptic signal by network via User Datagram Protocol (UDP). Finally, the receiving-end combines both haptic and visual signals for a more immersive telepresence, where another user can watch the scene in real time and also feels the haptic sensing via a haptic device.

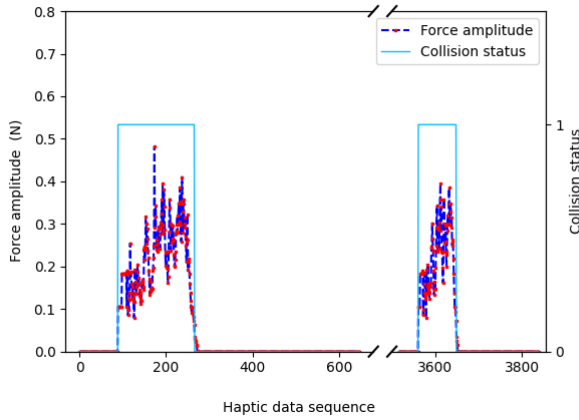


Figure 2: An example of haptic-visual correlations

The haptic and visual signals should be fully synchronized under normal conditions. Based on this simulation platform, we can observe the sequential correlation between haptic and visual signals. As shown in Fig. 2, there exists strong haptic signal fluctuations when the virtual hand (i.e. the ball) is on collision with another object. When the virtual hand visually touches the box, the force amplitude of haptic changes simultaneously. As the two objects are closer, the force amplitude is also higher; and vice versa. The force amplitude recovers to a constant when all objects are detached. These changes are also intuitive to the human users when operating a haptic-aware handle.

This intrinsic correlation inspires us to design a synchronization strategy. A sharp increase of force amplitude indicates a collision between the virtual hand and another object, while a sharp decrease implies a detachment between objects. If these deductions are inconsistent with the machine vision, we can conclude that there exists an asynchronization between haptic and visual signals and thus change the signal flows.

4 PROPOSED METHOD

Based on the above analysis, we propose the timestamp-independent synchronization method as shown in Fig. 3. Firstly, we extract the key samples in haptic signal where the amplitude is intensively

increased from near zero. Secondly, we extract the key frames in visual signal where the visual collision happens. Thirdly, we compare the time intervals of these key samples/frames to detect asynchronization phenomena. If a pair of time intervals (namely T_h and T_v) are with a large difference, the haptic-visual asynchronization is found and further fixed. Note here the object collision frequencies are low in real world, therefore, we can easily identify different pairs of time intervals. In the following subsections, the key sample detection, key frame detection, threshold selection, asynchronization removal and the overall method are elaborated, respectively.

4.1 Key sample detection in haptic signal

For haptic signal, the key samples are easily obtained for it consists of three one-dimensional signals (in x-axis, y-axis and z-axis). A sharp increase of force amplitude is found when its difference in any dimension is larger than a threshold (namely F_{th}). In this work, F_{th} is empirically set as 0.05. In additions, to reduce the effects of noise, we employ a Gaussian filter with kernel size 5 as a pre-processing of haptic signal.

An example of this step is shown in Fig. 4. An operation with force signals in three dimensions is presented, where all sharp increases are successfully detected and labeled as key samples. Correspondingly, their time intervals (i.e. T_h) are recorded for further comparison.

4.2 Key frame detection in visual signal

The objective of key frame detection is to find the time intervals when the virtual hand touches the box. Essentially, it consists of two modules: object detection and collision detection. The first module identifies all objects, while the second module determine whether object collision occurs. Both modules are achieved by computer vision methods.

4.2.1 Object detection: We select the popular YOLO network to recognize all objects in the video. With deep network, the YOLO network extracts the deep features of different objects and scenarios, thereby achieving object recognition with high accuracy. In particular, we employ the V3 of YOLO network [4] by jointly considering the efficiency and complexity.

We established our image database for training the YOLO V3 network. We acquired 1000 images from visual signals with an image size of 1600×900 pixels. Then the images were labeled via a label making tool (the application software of labellmg). We used rectangle to bound the balls in the images and labeled them as "ball", and accordingly, bound the boxes and labeled them as "box". All the labels were saved with xml files for using during training. The 800 images in this database are employed as the training set and the other 200 images are the test set.

The loss function plays an important role in the YOLO network. In this work, the position information of the ball and box are the target of the network. Therefore, the target's error of center coordinate in the form of squared difference is first taken into account in the loss function; then, in order to obtain the accurate bounding rectangle, the wide and high coordinate error in the form of cross-entropy is utilized; finally, as the detection of multiple categories of targets (ball and box) are involved, the category error in the form of cross-entropy must be considered. Hence, the loss function used

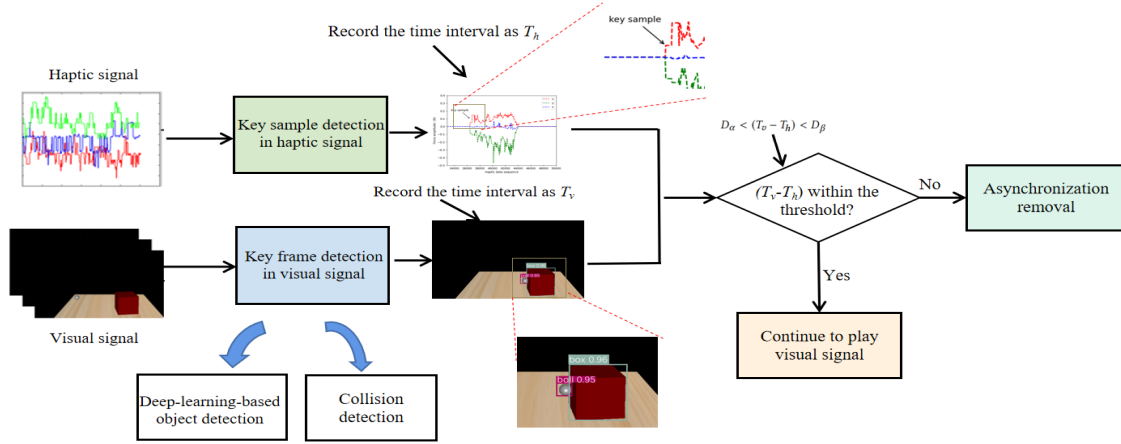


Figure 3: The flowchart of our proposed method

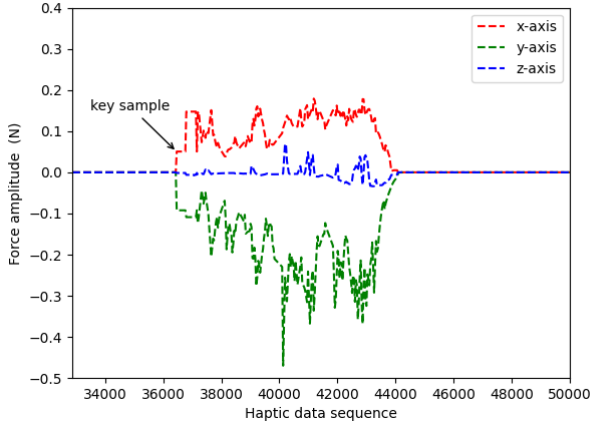


Figure 4: An example of key sample detection

in this work is:

$$\begin{aligned}
 Loss = & \lambda_{coord} \sum_{i=0}^{S^2} \sum_{j=0}^B I_{ij}^{obj} [(x_i - \hat{x}_i)^2 + (y_i - \hat{y}_i)^2] + \\
 & \lambda_{coord} \sum_{i=0}^{S^2} \sum_{j=0}^B I_{ij}^{obj} [(\sqrt{w_i} - \sqrt{\hat{w}_i})^2 + (\sqrt{h_i} - \sqrt{\hat{h}_i})^2] - \\
 & \sum_{i=0}^{S^2} \sum_{j=0}^B I_{ij}^{obj} [\hat{C}_i \log(C_i) + (1 - \hat{C}_i) \log(1 - C_i)] - \\
 & \lambda_{noobj} \sum_{i=0}^{S^2} \sum_{j=0}^B I_{ij}^{noobj} [\hat{C}_i \log(C_i) + (1 - \hat{C}_i) \log(1 - C_i)] - \\
 & \sum_{i=0}^{S^2} \sum_{c \in classes} I_{ij}^{obj} [\hat{P}_i \log(P_i) + (1 - \hat{P}_i) \log(1 - P_i)]
 \end{aligned} \quad (1)$$

Table 1: The hyperparameter settings in model training

epoch	batchsize	λ_{coord}	λ_{noobj}	learning rate
300	16	0.5	0.5	cosine decay

where the first row indicates the error of the center coordinates, S represents the grid size, B represents the bounding rectangle. I_{ij}^{obj} denotes whether targets are in the rectangle at grid (i, j) , and 0 vice versa. x_i and y_i represent the true center coordinates, \hat{x}_i and \hat{y}_i represent the predicted center coordinates. The second row represents the error of the width and height of the predicted rectangle, in which w_i and h_i represent the true width and height, \hat{w}_i and \hat{h}_i represent the predicted width and height. The third and fourth rows indicate the error of the confidence level, where C_i denotes the true confidence level, and \hat{C}_i denotes the predicted confidence level. The fifth row denotes the error of classification, where P_i and \hat{P}_i denote the true and the predicted categories, respectively. λ_{coord} and λ_{noobj} are the weights which will be trained as hyperparameters of network.

The main hyperparameters used in training are set as shown in Table 1. Among them, the learning rate is set as cosine decay as follows:

$$lr = [1 + \cos(x \times \frac{\pi}{2 \times epoch})] \times 0.95 + 0.05. \quad (2)$$

With this method, the training module has larger learning rate at the beginning to accelerate the training speed, and then the learning rate decreases with the increasing number of training epochs to more easily find the optimal solution. Experimental results show with our training strategy, the loss function converges to a very low level and is almost stable after 300 epochs of training.

After training, an example of recognition result is shown in Fig. 5, in which the virtual hand (i.e. the ball) and the box are detected, with their borders labeled by rectangular frames.

4.2.2 Collision detection: We determine whether a collision happens based on the aforementioned rectangular frames. Let (X_1, Y_1) and (X_2, Y_2) denote the top-left locations of virtual hand (i.e. the ball) and any object as target in 2D space, and (H_1, W_1) and (H_2, W_2) denote the sizes of corresponding rectangular frames, the condition of no collision is:

$$(Y_1 + H_1 > Y_2) \vee (X_1 + W_1 < X_2) \vee (Y_1 < Y_2 + H_2) \vee (X_1 > X_2 + W_2). \quad (3)$$

Otherwise, the collision of objects is found. At the time of collision found, we extract the corresponding video frame as the key frame of visual signal and record the time interval as T_v , which is further utilized for asynchronization detection.

4.3 The synchronization threshold

During haptic-visual delivery and playback, we can easily identify each key sample/frame pair considering the corresponding time intervals are usually very close to each other. For a pair of time intervals T_h and T_v , their difference is set as a criterion of haptic-visual asynchronization. A synchronization of signals is guaranteed if:

$$D_\alpha < (T_v - T_h) < D_\beta, \quad (4)$$

where D_α and D_β refer the lower and upper bound of perception threshold.

As results from subjective test can be more consistent with users' perception experience, we design an subjective test to determine D_α and D_β . Our test strictly follows the subjective test manual ITU-R BT.500 [24] with the following steps. First of all, we recruit 21 testees without prior knowledge of haptic coding or delivery. Then, we use the 2-alternative force choice method to perform the test. Each session of test consists of two randomly presented haptic-visual segments: with and without delay. The delay can be negative or positive with a range from -100ms to 100ms with an interval of 20ms. Each testee is asked to choose one segment that he/she cannot feel delay between the two. Finally, for each session, the probability of correct choices, which is obtained by Eq. (5), is recorded.

$$p_i = \frac{n_i}{N}, \quad (5)$$

where n_i denotes the number of testees who are make a correct choice in the i -th delay. N denotes the total number of testees.

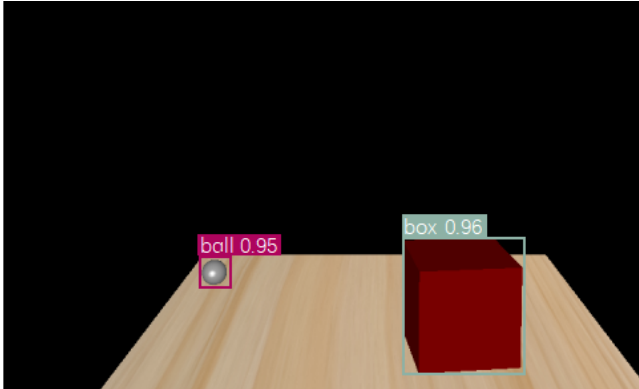


Figure 5: An example of object detection

As shown in Fig. 6, the probability of correct choices is around 0.5 when the delay of visual signals ranges from -60ms to 80ms. In other words, the human users cannot perceive the difference between delayed and non-delayed signals in this range. Therefore, we set the threshold of synchronization as $D_\alpha = -60ms, D_\beta = 80ms$.

4.4 Asynchronization removal

To adjust the signal stream and remove asynchronization phenomena, a general method is to select a main stream and set the remaining as auxiliary streams. When asynchronization occurs, all auxiliary streams are adjusted to be synchronized with the main stream. As reported in [27], the human perception of haptic signals is very sensitive that only the haptic signals above 1kHz provide smooth experience to users. This frequency is significantly higher than visual signals. Based on this fact, we utilize the haptic signal and visual signal as the main stream and the auxiliary stream, respectively. For synchronization, the visual signal is moved to be consistent with the haptic signal.

In multimedia communication system, the receiving-end usually set a buffer zone to cache all multimedia data for a smooth display of them. Therefore, if the visual signal is delayed more than D_α , we will retrieve the correct video frame from the buffer zone (i.e. take the next frame until synchronization status is judged); otherwise, if the visual signal is ahead by D_β , we will repeat the current frame until haptic-visual synchronization. Through this method, we are able to remove all asynchronization phenomena during haptic-visual delivery and playback.

4.5 The overall method

By summarizing Section 4.1-4.4, the detailed steps of our method are presented as follows.

Step 1. Initialization. Set a buffer zone at the receiving-end to cache haptic-visual data. Start the haptic-visual data delivery and playback. Go to Step 2.

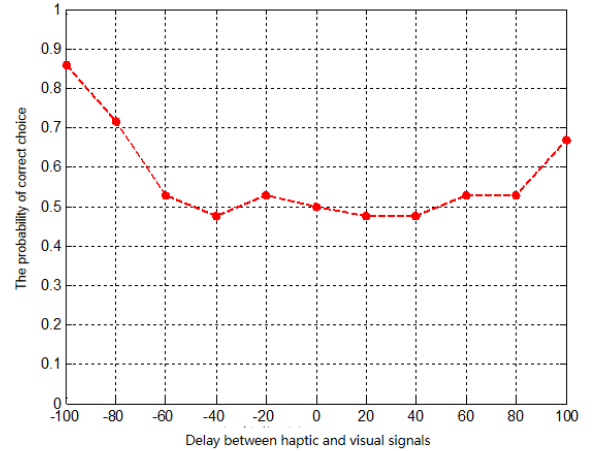


Figure 6: Subjective results of synchronization threshold

Step 2. Key sample detection. Keep to detect the key samples of haptic signals with the method in Section 4.1. If a key sample is found, set the time interval as T_h and go to Step 3.

Step 3. Key frame detection. Use the method in Section 4.2 to detect the corresponding key frames in the buffer and subsequent video of 1s. If a key frame is found, set the time interval as T_v and go to Step 4; otherwise, the synchronization detection fails, go to Step 2.

Step 4. Asynchronization examination. If Eq. (4) of Section 4.3 is true, go to Step 2 to check the following signals; otherwise go to Step 5.

Step 5. Asynchronization removal. Adjust the haptic-visual streams with the method shown in Section 4.4. Go to Step 2 to check the following signals.

5 EXPERIMENTAL RESULTS

To examine the effectiveness of proposed method, we implement it on the simulation platform shown in Section 3 and conduct both objective and subjective experiments. The frequencies of haptic and visual signals are set as 1000 Hz and 30 Hz, respectively. Due to the lack of haptic-visual synchronization method, we compare our model with the original case only.

5.1 Estimation accuracy of synchronization delay

The proposed method utilizes the synchronization delay $T_v - T_h$ to determine whether asynchronization happens. Therefore, the estimation accuracy of synchronization delay is critical in our method. We design the following experiment to examine the accuracy.

Based on the simulation platform, we randomly captured 100 haptic-visual clips, with the length of each clip as 30s. In other words, there exist 30000 haptic samples and 900 video frames in each clip, and totally exist 3 million haptic samples and 90000 video frames). For each haptic-visual clip, we add a random delay on visual signals. The delay is in the range of $[-330\text{ms}, 330\text{ms}]$ where the positive/negative values indicate visual signal is ahead/behind haptic signal. At the receiving-end, we employ our model to calculate the synchronization delay (namely \hat{x}) and compare it with the "actual" delay (namely x). The Mean Absolute Error (MAE) and Maximum Absolute Error (MaxAE) are utilized to be assessment metrics, in which MAE is calculated by:

$$MAE = \frac{1}{M} \sum_{i=1}^M |\hat{x}_i - x_i|, \quad (6)$$

where M is the total number of samples.

The results are shown in Table 2. From the table, the MAE and MaxAE values are 7.3 ms and 15 ms, respectively. It is noted that the haptic-visual synchronization is unperceivable in $[-60\text{ ms}, 80\text{ ms}]$, where the ratio of MAE and MaxAE are only 5.2% and 10.7%, respectively. On the other hand, the frame length of each video frame is $\frac{1}{30}\text{Hz} = 33.3\text{ ms}$, which is also significantly larger than the MAE/MaxAE values. Therefore, the estimation accuracy could fulfill the requirement in the practical applications of haptic-visual system.

Table 2: The estimation accuracy of $T_v - T_h$

Metrics	MAE(ms)	MaxAE (ms)
Results	7.3	15

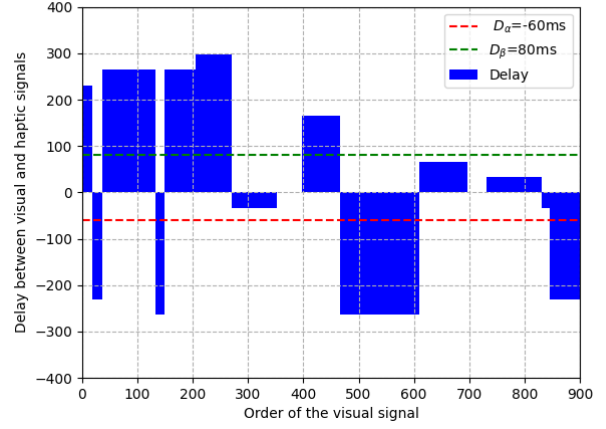


Figure 7: An example of random delay in the experiment

5.2 Effectiveness of haptic-visual synchronization

To evaluate the effectiveness of our synchronization detection and removal method, we examine it on the same dataset presented in Section 5.1.

At the sending end, after sending random video frames (in the range of $[0, 100]$), we add a random delay (in the range of $[-330\text{ms}, 330\text{ms}]$ and denoted as t_n) on it. We repeat the above process until all the frames in each chip (totally 100 clips) are sent. Considering that the proposed asynchronization removal method adjusts visual signal frame by frame, the interval of the above random delay is set the same as the frame interval of visual signal (i.e. 33ms). Therefore, the delay range of $[-330\text{ms}, 330\text{ms}]$ is equivalent to delay random number (denoted as d_n) of video frames in the range of $[-10, 10]$. Taking a clip (900 frames) as example, the random numbers generated in the experiment are shown in Table 3. In the table, the values in the first column indicate that the visual signal is ahead of the haptic signal $7 \times 33=231\text{ms}$ and the delay status lasts for $19 \times 33=627\text{ms}$. The above random delay in the experiment also intuitively shown in Fig. 7, in which the vertical axis indicates the delay between visual and haptic signals and the horizontal axis indicates the order of the visual signal. From the figure, the delays are random and representative to evaluate our method.

At the receiving end, we compare the probabilities of successful synchronization with and without our method. The results are presented in Table 4. By using our model, the average probability of synchronization increases from 25.3% to 89.2%. It should be pointed out that our synchronization method is executed frame by frame. If the haptic-visual delay is larger than 1 frame, the signal is kept asynchronized during the synchronization process. That is the

Table 3: An example of random delay in the experiment

d_n	7	-7	8	-8	8	9	-1	0	5	-8	-8	2	0	1	-1	-7
t_n	19	18	95	17	56	65	82	46	69	96	47	86	36	99	14	55

Table 4: Probabilities of synchronization with and without our method

	Without our method	With our method
Probabilities	25.3%	89.2%

reason why there are still 10.8% signals asynchronized in Table 4. Even at this scenario with severe fluctuations, our method still achieve a high probability of 89.2%, which reveals the effectiveness and robustness of our method in haptic-visual synchronization. The utilization of our model guarantees the signal synchronization in most cases, thereby greatly improving the system performance of haptic-visual interaction.

5.3 Subjective test on user experience

Besides of objective evaluation, we also conduct subject test to evaluate the improvement of user experience by our model. As mentioned in Section 1, the signal asynchronization is a critical factor to influence user experience in haptic-visual interaction. Therefore, the improvement of user experience can be taken as circumstantial evidence of the effectiveness of our model.

We recruit 23 testees to participate this test, where all haptic-visual sequences are also the same to those in Section 5.1. To calculate the correlations, we introduce the delays that are evenly distributed from -10 to 10 frames (that is, ranged from -333 ms to 333ms with the interval of 33.3ms) and occasionally utilize the proposed synchronization method at the receiving end. However, whether or not using the synchronization is unknown for all testees. As a result, a testee scores his/her experience based on the real feelings and experiences. All scores are between 0 and 10 and their averaged value, the Mean Opinion Score (MOS), represents the average perceptions of human users.

The collected subjective test results are pre-processed to remove outliers based on the ITU subjective test regulations. We calculate the correlations, including Pearson Linear Correlation Coefficient (PLCC) and Spearman Rank-Order Correlation Coefficient (SROCC) [22], between each testee's score and the MOS. The results are shown in Fig. 8. According to ITU-R BT.500 [24], a testee's score is considered as an outlier if the correlation between his/her score and the MOS is less than 0.7. Therefore, from Fig. 8, the 12th and 18th testees are considered as outliers and subsequently excluded in the final results.

The scores of the remaining 21 testees are further examined by data saturation validation [13]. Due to randomness of user scores, insufficient testees would lead to inaccurate MOS values. To check whether the testees are enough, the data saturation validation was proposed. For a subjective test with K testees, it randomly selects $k = 1, 2, \dots, K$ testees to calculate the correlation between their averaged score and the MOS. If the correlation value converges to 1

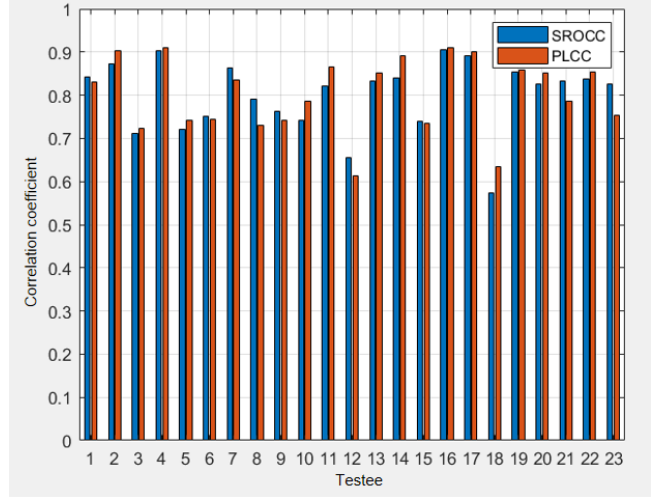


Figure 8: The correlations between each testee and the MOS

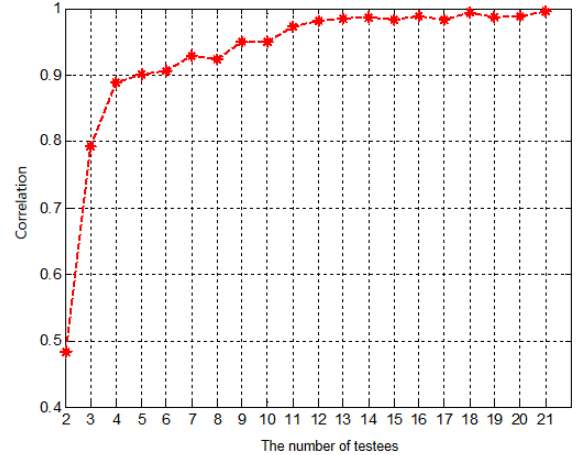


Figure 9: The data saturation validation in our test

as k increases, the testees are considered sufficient. In our test, this correlation value is very close to 1 with $k = 13$ testees, as shown in Fig. 9. Therefore, the remaining 21 testees are sufficient to represent the averaged opinion of human users.

Fig. 10 shows the MOS values under different delay settings. Two settings are compared: receiving end with and without our method. In the central part of curves (i.e. -33 ms 66 ms), the delays are unperceivable to human users and thus the two settings achieve very similar MOS values. As the absolute value of delay gets larger,

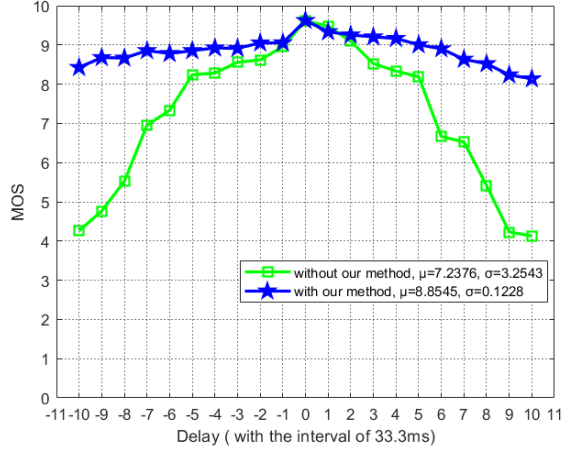


Figure 10: The subjective improvements with our method

the difference between the two settings becomes more significant. In extreme cases (i.e. ± 330 ms), our synchronization method improves the MOS values by around 4, which shows the high capability of anti-interference under severe network conditions. On average, the MOS value is increased by 1.6169, with MOS variation decreased by 3.1315. This fact demonstrates the significant improvement of our synchronization method that is agreed by the majority of human users. In conclusion, the proposed method can guarantee the user experience in case of haptic-visual asynchronization.

6 CONCLUSIONS

In this paper, we exploited the haptic-visual correlations in haptic-aware interaction system. Based on the observations, we proposed a timestamp-independent synchronization method for haptic-visual signals, which consists of haptic signal analysis, learning-based vision analysis, perception-based thresholding and an overall method for asynchronization detection and removal. It should be pointed out that the referring of virtual hand (i.e. the ball) and target (i.e. the box) can be extended to more types of objects with retrained models. Therefore, our model is still applicable in more general scenarios. To our best knowledge, this is the very first attempt to design a haptic-aware multimedia synchronization model by considering the special characteristics of haptic interaction. It can also be utilized as a reference to design new synchronization models for emerging sensorial media such as olfaction signals. We envision a more widespread use of multiple sensorial media that benefits the immersive user experience in the foreseeable future.

REFERENCES

- [1] Adnan Aijaz, Mischa Dohler, A. Hamid Aghvami, Vasilis Friderikos, and Magnus Frodigh. 2017. Realizing the Tactile Internet: Haptic Communications over Next Generation 5G Cellular Networks. *IEEE Wireless Communications* 24, 2 (2017), 82–89. <https://doi.org/10.1109/MWC.2016.1500157RP>
- [2] Konstantinos Antonakoglou, Xiao Xu, Eckehard Steinbach, Toktam Mahmoodi, and Mischa Dohler. 2018. Toward Haptic Communications Over the 5G Tactile Internet. *IEEE Communications Surveys Tutorials* 20, 4 (2018), 3034–3059. <https://doi.org/10.1109/COMST.2018.2851452>
- [3] Su Thandar Aung, Yutaka Ishibashi, Khin Than Mya, Hitoshi Watanabe, and Pingguo Huang. 2020. Influences of Network Delay on Cooperative Work in Networked Virtual Environment with Haptics. In *2020 IEEE REGION 10 CONFERENCE (TENCON)*. 1266–1271. <https://doi.org/10.1109/TENCON50793.2020.9293934>
- [4] Haipeng Chen, Zhentao He, Bowen Shi, and Tie Zhong. 2019. Research on Recognition Method of Electrical Components Based on YOLO V3. *IEEE Access* 7 (2019), 157818–157829. <https://doi.org/10.1109/ACCESS.2019.2950053>
- [5] E. Dong. 2019. *Application of Haptic Virtual Fixtures on Hot-Line Work Robot-Assisted Manipulation*. Intelligent Robotics and Applications.
- [6] Varun S.I. Durai, Raj Arjunan, and M. Manivannan. 2019. The Effect of Audio and Visual Modality Based CPR Skill Training with Haptics Feedback in VR. In *2019 IEEE Conference on Virtual Reality and 3D User Interfaces (VR)*. 910–911. <https://doi.org/10.1109/VR.2019.8798006>
- [7] Mohamed El-Helaly and Aishy Amer. 2007. Synchronization of Processed Audio-Video Signals using Time-Stamps. In *2007 IEEE International Conference on Image Processing*, Vol. 6. VI – 193–VI – 196. <https://doi.org/10.1109/ICIP.2007.4379554>
- [8] Vpd Fonseca, Bmr Lima, Tead Oliveira, Q. Zhu, and E. M. Petriu. 2019. In-Hand Telemanipulation Using a Robotic Hand and Biology-Inspired Haptic Sensing. In *2019 IEEE International Symposium on Medical Measurements and Applications (MeMeA)*.
- [9] BD Gwenaëlle and C. Caroline. 2019. A touch of gloss: haptic perception of packaging and consumers' reactions. *Journal of Product and Brand Management* 28, 1 (2019), 117–132.
- [10] J. W. Hong, K. K. Wei, Aiy Chan, S. J. Omamalin, and Aiba Rahim. 2019. *Deformation and Friction: 3D Haptic Asset Enhancement in e-Commerce for the Visually Impaired*. Haptic Interaction, Perception, Devices and Algorithms.
- [11] B. Ilaria, L. Daniele, M. Nicola, C. Alessandra, B. Luca, P. Caterina, S. Massimiliano, and F. Antonio. 2018. Wearable Haptics and Immersive Virtual Reality Rehabilitation Training in Children With Neuromotor Impairments. *IEEE Transactions on Neural Systems and Rehabilitation Engineering* 26 (2018), 1469–1478.
- [12] Toshiaki Kikuchi and Yuko Ozasa. 2018. Watch, Listen Once, and Sync: Audio-Visual Synchronization With Multi-Modal Regression Cnn. In *2018 IEEE International Conference on Acoustics, Speech and Signal Processing (ICASSP)*. 3036–3040. <https://doi.org/10.1109/ICASSP.2018.8461853>
- [13] Chao Li, Hui Yang, Bowen Bao, Huifeng Guo, Yong Jiang, and Jie Zhang. 2020. Spearman Correlation Coefficient Abnormal Behavior Monitoring Technology Based on RNN in 5G Network for Smart City. In *2020 International Wireless Communications and Mobile Computing (IWCMC)*. 1440–1442. <https://doi.org/10.1109/IWCMC48107.2020.9148469>
- [14] S. Li, R Rameshwar, A. M. Votta, and C. D. Onal. 2019. Intuitive Control of a Robotic Arm and Hand System With Pneumatic Haptic Feedback. *IEEE Robotics and Automation Letters* PP, 99 (2019), 1–1.
- [15] Tommaso Lisini Baldi, Stefano Scheggi, Marco Aggravi, and Domenico Praticchizzo. 2018. Haptic Guidance in Dynamic Environments Using Optimal Reciprocal Collision Avoidance. *IEEE Robotics and Automation Letters* 3, 1 (2018), 265–272. <https://doi.org/10.1109/LRA.2017.2738328>
- [16] Yangjun Qiao, Quanfei Zheng, Yuting Lin, Ying Fang, Yiwen Xu, and Tiesong Zhao. 2020. Haptic Communication: Toward 5G Tactile Internet. In *2020 Cross Strait Radio Science Wireless Technology Conference (CSRSWTC)*. 1–3. <https://doi.org/10.1109/CSRSWTC50769.2020.9372659>
- [17] Regunathan Radhakrishnan, Kent Terry, and Claus Bauer. 2008. Audio and video signatures for synchronization. In *2008 IEEE International Conference on Multimedia and Expo*. 1549–1552. <https://doi.org/10.1109/ICME.2008.4607743>
- [18] Shree Krishna Sharma, Isaac Woungang, Alagan Anpalagan, and Symeon Chatzinotas. 2020. Toward Tactile Internet in Beyond 5G Era: Recent Advances, Current Issues, and Future Directions. *IEEE Access* 8 (2020), 56948–56991. <https://doi.org/10.1109/ACCESS.2020.2980369>
- [19] Nicolas Staelens, Jonas De Meulenaere, Lizzy Bleumers, Glenn Van Wallendael, Jan De Cock, Koen Geeraert, Nick Vercammen, Wendy Van den Broeck, Brecht Vermeulen, Rik Van De Walle, and Piet Demeester. 2012. Assessing the Importance of Audio/Video Synchronization for Simultaneous Translation of Video Sequences. *Multimedia Systems* 18, May 2012 (3 5 2012), 445–457.
- [20] N. Staelens, J. D. Meulenaere, L. Bleumers, G. V. Wallendael, J. D. Cock, K. Geeraert, N. Vercammen, Wvd Broeck, B. Vermeulen, and Rvd Walle. 2012. Assessing the importance of audio/video synchronization for simultaneous translation of video sequences. *Multimedia Systems* 18, 6 (2012), 445–457.
- [21] Eckehard Steinbach, Matti Strese, Mohamad Eid, Xun Liu, Amit Bhardwaj, Qian Liu, Mohammad Al-Ja'afreh, Toktam Mahmoodi, Rania Hassen, Abdulmotaleb El Saddik, and Oliver Holland. 2019. Haptic Codecs for the Tactile Internet. *Proc. IEEE* 107, 2 (2019), 447–470. <https://doi.org/10.1109/JPROC.2018.2867835>
- [22] Chandrasegar Thirumalai, Swapna Anupriya Chandhini, and M Vaishnavi. 2017. Analysing the concrete compressive strength using Pearson and Spearman. In *2017 International conference of Electronics, Communication and Aerospace Technology (ICECA)*, Vol. 2. 215–218. <https://doi.org/10.1109/ICECA.2017.8212799>
- [23] A. Torfi, S. M. Iranmanesh, N. Nasrabadi, and J. Dawson. 2017. 3D Convolutional Neural Networks for Cross Audio-Visual Matching Recognition. *IEEE Access* PP, 99 (2017), 1–1.
- [24] International Telecommunication Union. 2002. *Methodology for the Subjective Assessment of the Quality of Television Pictures*.
- [25] Y. Xu, Y. Huang, W. Chen, H. Xue, and T. Zhao. 2019. Error Resilience of Haptic Data in Interactive Systems. In *2019 11th International Conference on Wireless Communications and Signal Processing (WCSP)*.
- [26] Ming Yang, Nikolaos Bourbakis, Zizhong Chen, and Monica Trifas. 2007. An Efficient Audio-Video Synchronization Methodology. In *2007 IEEE International Conference on Multimedia and Expo*. 767–770. <https://doi.org/10.1109/ICME.2007.4284763>
- [27] Yutaka Ishibashi, Mya Sithu, and Pingguo Huang. 2018. *Media Synchronization in Networked Multisensory Applications with Haptics*.
- [28] Qi Zeng, Yutaka Ishibashi, Norishige Fukushima, Shinji Sugawara, and Kostas E. Psannis. 2013. Influences of inter-stream synchronization errors among haptic media, sound, and video on quality of experience in networked ensemble. In *2013 IEEE 2nd Global Conference on Consumer Electronics (GCCE)*. 466–470. <https://doi.org/10.1109/GCCE.2013.6664891>
- [29] Hailing Zhou, Lei Wei, Ran Cao, Samer Hanoun, Asim Bhatti, Yonghang Tai, and Saeid Nahavandi. 2018. The Study of Using Eye Movements to Control the Laparoscope Under a Haptically-Enabled Laparoscopic Surgery Simulation Environment. In *2018 IEEE International Conference on Systems, Man, and Cybernetics (SMC)*. 3022–3026. <https://doi.org/10.1109/SMC.2018.00513>